J Neurosurg: Spine 3:142–148, 2005

A novel intramedullary spinal cord tumor model: functional, radiological, and histopathological characterization

GAURAV MAVINKURVE, B.S., GUSTAVO PRADILLA, M.D., FEDERICO G. LEGNANI, M.D., BETTY M. TYLER, B.A., CARLOS A. BAGLEY, M.D., HENRY BREM, M.D., AND GEORGE JALLO, M.D.

Departments of Neurosurgery, Pediatrics, and Oncology, The Johns Hopkins University School of Medicine, Baltimore, Maryland; and Ospedale San Gerardo, Monza, Italy

Object. Survival rates for high-grade intramedullary spinal cord tumors (IMSCTs) are approximately 30%, and optimal therapy has yet to be determined. Development of a satisfactory intramedullary tumor model is necessary for testing new therapeutic paradigms that may prolong survival. The authors report the technique, functional progression, radiological appearance, and histopathological features of a novel intramedullary model in rabbits.

Methods. Ten New Zealand white rabbits were randomized to receive an intramedullary injection of either 25 μl of VX2 carcinoma cells (500,000 cells; six rabbits) or 25 μl of medium (Dulbecco modified Eagle medium; four rabbits) into the midthoracic spinal cord. Postoperatively the rabbits were evaluated twice daily for neurological deficits. High-resolution magnetic resonance (MR) images were acquired preoperatively and weekly postoperatively until onset of paraparesis, at which point the animals were killed, and the midthoracic spines were processed for histopathological examination.

The VX2-carcinoma cells grew in 100% of animals injected and resulted in a statistically significant mean onset of paraparesis of 16.8 ± 1.7 days ($p = 0.0035$, log-rank test), compared with animals in the control group in which neurological deficits were absent by Day 45. Contrast-enhanced T_1-weighted MR imaging best demonstrated space-occupying intramedullary lesions and histopathological findings confirmed the intramedullary location of the tumor. Animals in the control group exhibited no functional, radiographic, or pathological signs of tumor.

Conclusions. Progression to paraparesis was consistent in all the VX2-injected animals, with predictable onset of paraparesis occurring approximately 17 days postinjection. Histopathological and radiological characteristics of the VX2 intramedullary tumor are comparable with those of aggressive primary human IMSCTs. Establishment of this novel animal tumor model will facilitate the testing of new therapeutic paradigms for the treatment of IMSCTs.

KEY WORDS • intramedullary tumor • spinal cord • animal model • VX2 • rabbit

INTRAMEDULLARY spinal cord tumors are rare lesions that comprise approximately 6 to 8% of all CNS tumors.[4] The three most common types of IMSCTs are ependymomas, low-grade astrocytomas, and high-grade astrocytomas.[4] Although most IMSCTs may be successfully treated with complete resection,[7–9] high-grade and inoperable tumors are associated with poor prognosis and the optimal treatment has yet to be determined.[6] Current treatment options for these high-grade and diffuse IMSCTs are limited to subtotal resection with or without adjuvant radiotherapy.[4,18,19,22,27] Despite multimodal adjuvant therapy, patients with malignant IMSCTs die of their disease within a relatively short period of time, usually within 2 years of diagnosis.

Although chemotherapy has been incorporated into the treatment of various intracranial neoplasms,[15,17] its role in IMSCTs remains undefined.[4] Systemic chemotherapeutic regimens have been used in the treatment of spinal cord astrocytomas, but their efficacy needs to be confirmed in larger studies.[1,3,11,16,23] The discovery of more potent and specific antineoplastic agents, and the development of novel drug delivery systems for CNS malignancies including controlled-release polymers and convection-enhanced delivery, among others, could be of benefit in the treatment of IMSCTs; however, adequate testing of these novel treatments requires a reproducible and accessible animal model of IMSCTs for preclinical testing.

In contrast to the abundance of intracranial animal tumor models,[5,10,14,26,28] the literature lacks a comprehensive animal model for IMSCTs, and development of such a model is a prerequisite for future investigations. An ideal animal model for this disease should be accessible; it should have a reproducible course of paraparesis onset with a predictable pattern of tumor infiltration and a therapeutic window adequate for experimental intervention; it must be amenable to neuroimaging monitoring; and it must resemble the infiltrative nature of human IMSCTs.

In the present study we describe a novel intramedullary tumor model in rabbits that were injected with VX2 carcinoma and report the onset of paraparesis, neuroimaging-do-

Abbreviations used in this paper: CNS = central nervous system; DMEM = Dulbecco modified Eagle medium; IMSC = intramedullary spinal cord tumor; MR = magnetic resonance.

cumented changes, and histopathological characteristics of the tumor model. To our knowledge, this is the first animal model of IMSCTs with a predictable onset of paraparesis, MR imaging characteristics, and histopathological data.

Materials and Methods

Experimental Design

Ten New Zealand White rabbits were randomized into two experimental groups. Animals in Group 1 (six rabbits) received a 25-μl intramedullary injection of 2.0×10^7 cells/ml (500,000 cells) of VX2 carcinoma in the midthoracic spinal cord. Animals in Group 2 (four rabbits) received a 25-μl injection of DMEM at the same level. The animals were followed by clinical and neuroimaging evaluations and were killed on onset of paraparesis, when spine specimens were harvested for histopathological analysis.

Animal Population

Male New Zealand white rabbits (*Oryctolagus cuniculus*; Robinson Services, Mocksville, NC) weighing between 2.2 and 3.7 kg (mean 2.9 kg) were used in this experiment. The rabbits were individually housed in standard facilities and given free access to Baltimore city water and rabbit chow. The experimental protocol was approved by the Animal Care and Use Committee of the Johns Hopkins University.

Tumor Cell Line

The VX2 squamous cell carcinoma (a generous gift from Dr. John Hilton, Department of Radiology, Johns Hopkins University, Baltimore, MD) was maintained by serial passage in carrier rabbits. To produce the cell suspension, approximately 0.5 g of fresh tumor tissue obtained from a carrier rabbit was minced and then incubated for 18 hours (5% CO_2 at 37°C) in 10 μl of dissociation medium consisting of 50 U/ml collagenase and 0.0005% DNAse in Roswell Park Memorial Institute media 1640 containing 10% fetal bovine serum and 60 mM 4-(2-hydroxyethyl)-1-piperazineethanesulfonic acid. The tumor was further dissociated by repeated pipetting, washed twice with Roswell Park Memorial Institute 1640/10% fetal bovine serum, and then centrifuged and resuspended in DMEM. Viable cells, determined by Trypan blue exclusion, were counted with a hemocytometer. Cells were diluted to 2.0×10^7 cells/ml in DMEM.

Surgical Technique

Animals were anesthetized with an intramuscular injection of a mixture of ketamine 50 mg/kg (100 mg/ml; Abbot Laboratories, Chicago, IL) and xylazine 10 mg/kg (100 mg/ml; Phoenix Pharmaceutical, St. Joseph, MO). The posterior thoracic region was shaved and prepared in a sterile fashion. A midline incision approximately 4 cm long was made over the midthoracic spine, and subperiosteal dissection of the paravertebral muscles was performed using electrocautery (Fig. 1). The spinous process and bilateral lamina of one midthoracic level (between T- 4 and T-5) were removed using rongeurs to expose the dura mater (Fig. 1 *center*). A 22-gauge Hamilton needle (Hamilton Co., Reno, NV) was inserted to a depth of 2 mm into the spinal cord (Fig. 1 *right*). As shown in Fig. 1 *right*, placing the needle at this depth allows injection of the cells into the center of the anteroposterior diameter of the spinal cord. The six rabbits in the tumor group received a 25-μl intramedullary injection of 2×10^7 cells/ml (500,000 cells) of VX2 carcinoma, whereas the four rabbits in the control group received a 25-μl intramedullary injection of DMEM (Table 1). To avoid a cerebrospinal fluid leak, the muscles, fascia, and skin were closed with suture in a standard fashion. After recovery, the animals were returned to their cages. Each animal was subsequently evaluated twice a day for any neurological deficits.

Imaging Analysis

All animals underwent high-resolution MR imaging preoperatively, weekly postoperatively, and immediately following onset of paraparesis. The MR images were acquired using a CV/i 1.5-tesla clinical unit (GE Medical Systems, Wausheka, WI) in which an extremity coil was used. The animals were sedated with an intramuscular mixture of ketamine 50 mg/kg and xylazine 10 mg/kg, and an intravenous line was placed in an ear vein for venous access. Sagittal and axial T_1- and T_2-weighted images were initially obtained. Gadolinium diethylentriaminepentaacidic acid dimeglumine (Magnevist; Berlex Laboratories, Wayne, NJ) at a dose of 0.1 mmol/kg was then injected intravenously, and the T_1-weighted images were acquired.

Histological Studies

The animals were killed promptly after onset of paraparesis or by 45 days if paresis had not occurred. Following administration of a 75-mg/kg and 15-mg/kg intramuscular injection of ketamine hydrochloride and xylazine, respectively, the thorax was rapidly opened, the right atrium was incised, and a cannula was inserted into the left ventricle. Normal saline followed by 10% paraformaldehyde was pumped through the animal's circulation. Following death, three levels of thoracic spine, centered on the site of the tumor cell injection, were dissected en bloc and placed in 10% paraformaldehyde. After 1 week's fixation, the spines were decalcified for 6 weeks and then sectioned and stained with H & E. The presence of tumor was assessed and the pattern of infiltration, the intrinsic tumor characteristics, and the effect of tumor presence on intramedullary structure were recorded.

Statistical Analysis

Statistical analysis included comparison of data pertaining to onset of paraparesis in tumor and control groups (log-rank test performed with JMP 5.1 [SAS Institute, Inc., Cary, NC]). The Kaplan–Meier curves of the two groups were graphically illustrated using Microsoft Excel 2000 (Microsoft, Redmond, WA). Probability values less than 0.05 were considered to be statistically significant.

Results

The VX2 tumor cells grew in 100% of animals in which the tumor cell suspension was injected and resulted in a statistically significant mean onset of paraparesis at 16.8 ± 1.7 days (0.0035, log-rank test) after tumor implantation, compared with animals in the control group in which neurological deficits remained absent by Day 45 (Fig. 2). Mild hindlimb weakness rapidly progressed to severe paraparesis within 12 hours, and urinary and fecal incontinence usually accompanied this event. Of the MR imaging sequences, T_1-weighted contrast-enhanced images best demonstrated space-occupying intramedullary lesions, with acute ischemic cord changes found in all animals injected with VX2 (Fig. 3). Histopathological analysis confirmed the intramedullary location of the tumor and showed sheets of neoplastic cells with extensive invasion and connection of the spinal cord (Fig. 4). Areas of marked ischemia and coagulative necrosis were seen within the tumor. Animals in the control group exhibited no functional neuroimaging, (Fig. 3 *upper* and *lower*), or pathological signs of tumor (Fig. 5).

Discussion

In the present study we describe a novel animal model of intramedullary spinal cord tumors in rabbits in which a single intramedullary injection of VX2 carcinoma was used. This tumor model will enable preclinical testing of novel treatment modalities, including local chemotherapy, radiotherapy, antiangiogenic and immunomodulatory approaches, and combination therapies.

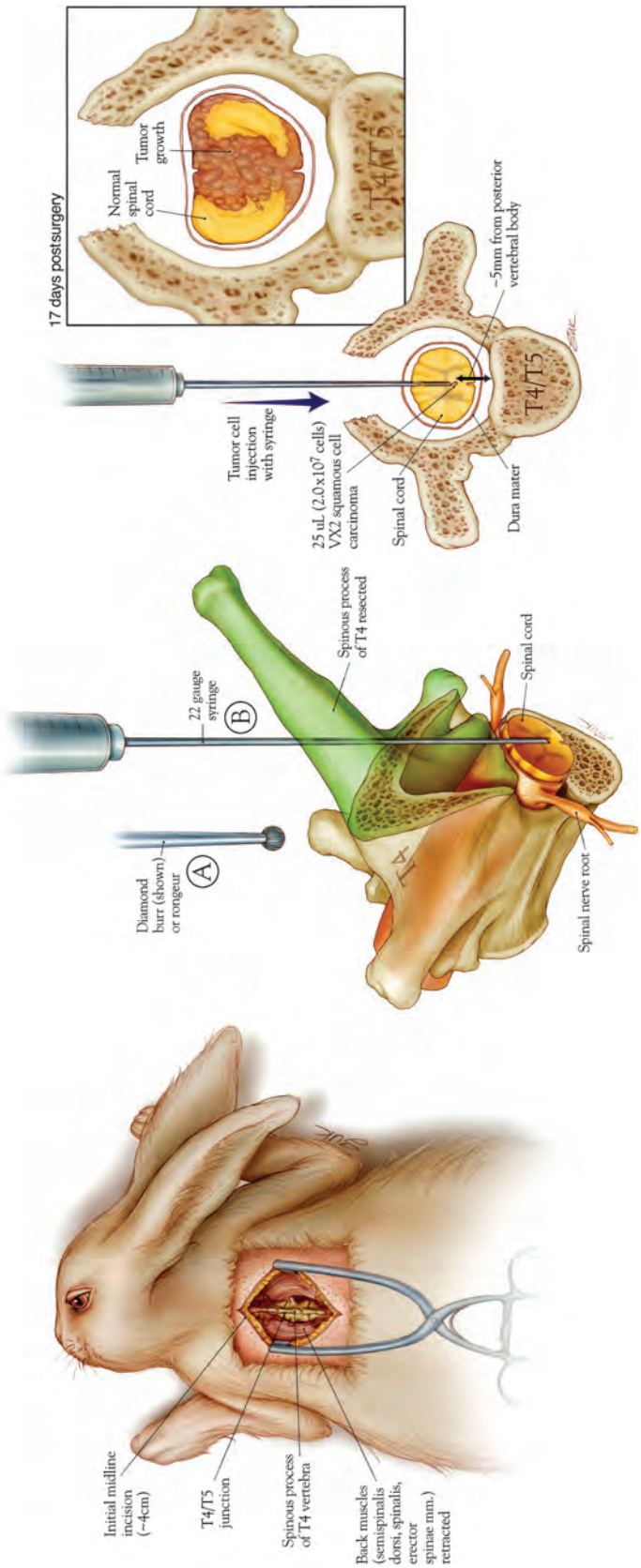

FIG. 1. Artist's illustrations. *Left:* The position of the rabbit, the level for tumor implantation, and anatomy of the thoracic spine. *Center:* The location of the spinous process that is resected (A), the trajectory of the needle (B), and the location of tumor implantation. *Right:* A transverse section of the thoracic spine demonstrating the appropriate location for tumor implantation; *inset* shows the macroscopic appearance of the tumor and its intramedullary location.

TABLE 1
*Summary of data obtained in 10 experimental rabbits**

Case No.	Animal Weight (kg)	Injection Content	No. of Days to Paraparesis
1	2.8	tumor	16
2	2.8	DMEM	—
3	3.7	tumor	14
4	2.6	tumor	17
5	2.2	DMEM	—
6	2.8	tumor	25
7	2.8	DMEM	—
8	2.9	DMEM	—
9	3.0	tumor	14
10	2.9	tumor	15

* DMEM = 25-μl intramedullary injection of DMEM; tumor = 25-μl injection of 2×10^7 cells/ml (500,000 cells) of VX2 carcinoma; — = not applicable.

In formulating an intramedullary tumor model, an animal's size was of particular interest because experimental treatment protocols involving spinal drug delivery systems and imaging techniques are optimized for humans. Therefore, animals larger than mice or rats were highly desirable. Furthermore, the implanted tumor had to be easily and reliably inducible and had to display classic malignant features. One of the few experimental tumor cells easily implantable in rabbits is VX2, a squamous cell carcinoma syngeneic to New Zealand white rabbits.[20] This tumor line has been used extensively to investigate antitumor treatments in different organs including breast,[2] lung,[12] liver,[13,21] and kidney.[24] Tumor induction occurred in all of these locations without an altered immune response and with a response rate greater than 80%. The growth rate is quite high, starting from a tumor volume of 10^6 cells to a tumor size of 2 cm within 3 to 4 weeks.

Our intramedullary tumor model met these expectations, with a 100% induction rate and a tumor size of approximately 1 cm in 17 days. As shown in Table 1, an outlier was present in the VX2 injection group. This animal experienced paraparesis 25 days after injection, whereas neurological deficits developed in 14 to 17 days after injection. Histopathological analysis of the spinal cord confirmed the presence of intramedullary tumor in this animal. The slower onset of paraparesis could be related to several factors including biological variability of the host, smaller concentration of cells in the aliquot, exposure of the aliquot to changes in temperature, and occlusion of the needle in the Hamilton syringe, among others. In our experience with animal models of intracranial gliomas in rodents, we have observed this phenomenon frequently; however, as it occurred in our rabbit model, only one animal in the experimental group usually exhibits this behavior—strictly controlling the concentration of the injected cells and the temperature of the aliquots, as well as verification of the adequate permeability of the needle prior to injection, usually decreases the likelihood of these events.

In a review of the literature we found only one previous intramedullary tumor model. In 1984, Salcman, et al.,[25] reported an intramedullary tumor model in adult mongrel dogs in which a tumor cell suspension (10^6 cells, volume 0.02–0.05 ml) had been injected at two to three sites in the thoracic spine. Paraparesis developed in six of 10 dogs, but its onset varied between 9 and 14 days with tumors failing to develop in two dogs. Several dogs underwent computerized tomography scanning and myelography, which demonstrated syringomyelia within the spinal cord.

Although this aforementioned study demonstrated a technique for intramedullary tumors, the onset of paresis was not reliable or consistent, and the advent of MR imaging warrants a new model. Furthermore, the rabbit is more amenable to preclinical testing than the dog, which weighed as much as 25 kg in the aforementioned experiment. Therefore, the rabbit intramedullary tumor model in which there is MR imaging characterization provides an optimal framework for rapid and large-scale preclinical testing of new treatment paradigms. Because MR imaging is the diagnostic study of choice for human IMSCTs, any animal model of these tumors must include MR imaging analysis. In the present study, MR imaging clearly demonstrated intramedullary lesions with edema or infiltrative signal characteristics comparable to certain high-grade human IMSCTs.

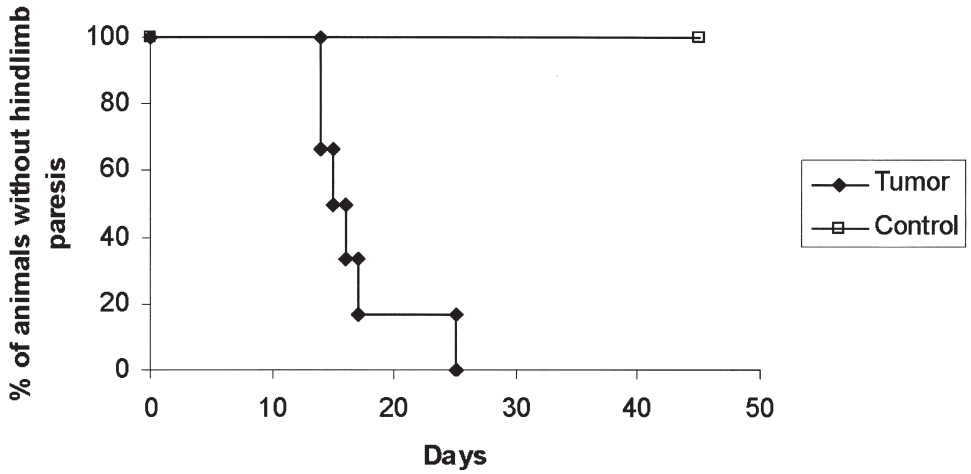

FIG. 2. Kaplan–Meier graph showing onset of paraparesis in tumor and control groups.

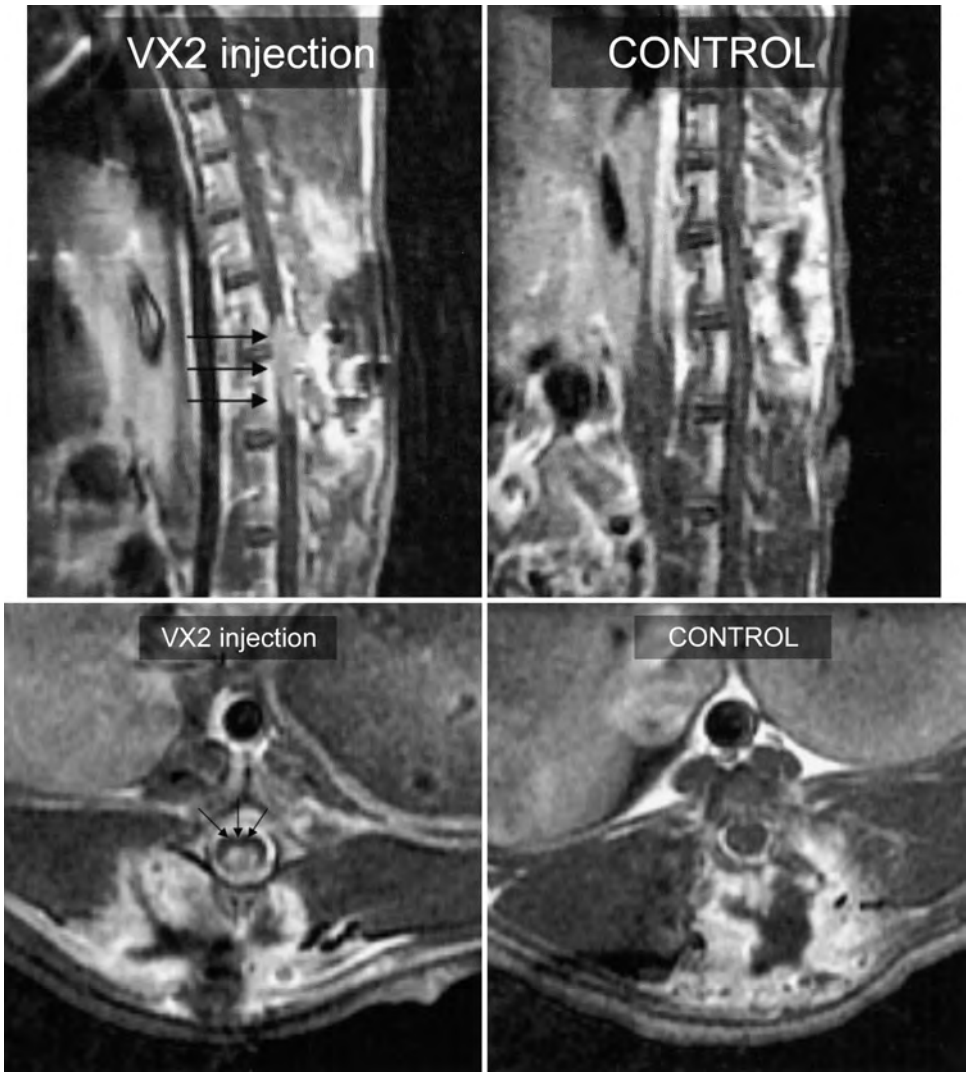

FIG. 3. *Upper:* Contrast enhanced MR images. Sagittal T_1-weighted images demonstrating intramedullary tumor in the thoracic spinal cord *(black arrows, left)* and the thoracic spinal cord of a control rabbit *(right)*. *Lower:* Axial T_1-weighted images revealing intramedullary tumor in the thoracic spinal cord *(black arrows; left)* and the thoracic spinal cord *(right)*.

The weaknesses of this model include the use of a squamous cell carcinoma line and the sample size. Whereas most human IMSCTs are of glial origin, VX2 has an epithelial origin; however, this limitation is quite unavoidable because VX2 is the only transplantable tumor cell line syngeneic to the rabbit and there is a general paucity of cell lines available for large animals. Nevertheless, VX2 shares some histological and neuroimaging features of high-grade intramedullary tumors and has been successfully used to model intracranial neoplasms.[5] Although the sample size for this experiment is small, a number of 10 was acceptable given the 100% induction rate observed in the VX2-injected animals and the lack of deficits seen in the controls. No additional animals were used to minimize suffering. Despite its limitations, this model has important applications including testing of novel treatment modalities such as stereotactic radiotherapy and local delivery of chemotherapy in a controlled experimental setting.

Although other CNS tumor models have been well studied, this is the first reliable and reproducible animal IMSCT model complete with MR imaging characterization. Clinical progression was consistent and predictable, and the techniques and materials used are widely accessible. Histopathological and neuroimaging characteristics of the intramedullary VX2 tumor are comparable with those of aggressive primary human IMSCTs. The establishment of this tumor model represents an important step in the path toward developing new treatment paradigms that may prolong survival in patients with spinal cord tumors.

Acknowledgment

We thank Ian Suk for his wonderful illustrations.

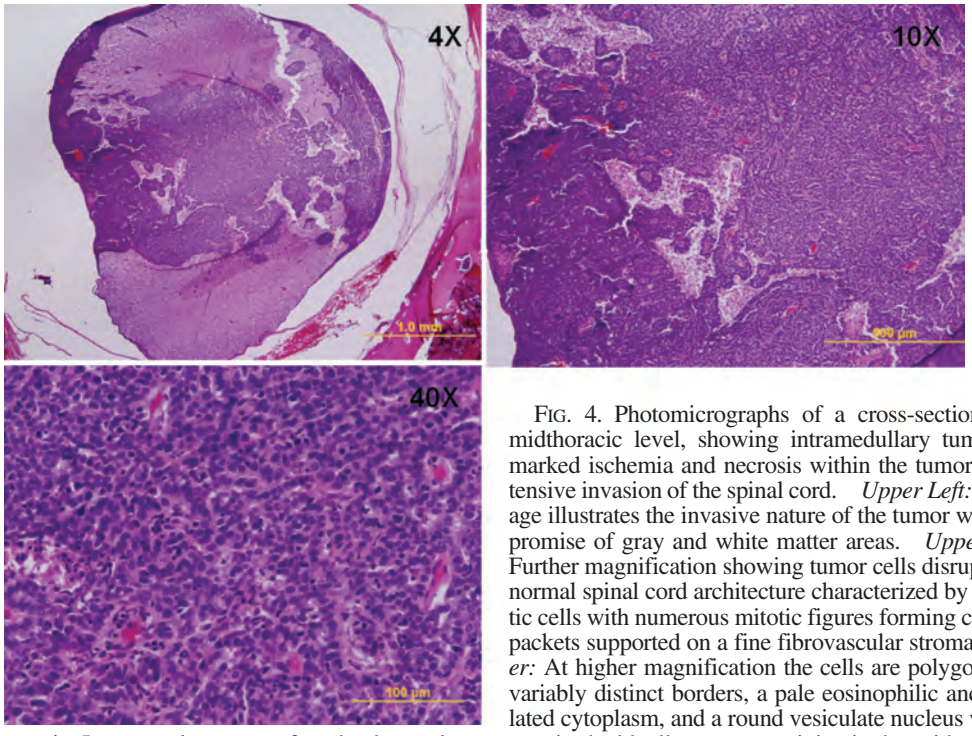

FIG. 4. Photomicrographs of a cross-section at the midthoracic level, showing intramedullary tumor with marked ischemia and necrosis within the tumor and extensive invasion of the spinal cord. *Upper Left:* The image illustrates the invasive nature of the tumor with compromise of gray and white matter areas. *Upper Right:* Further magnification showing tumor cells disrupting the normal spinal cord architecture characterized by anaplastic cells with numerous mitotic figures forming cords and packets supported on a fine fibrovascular stroma. *Lower:* At higher magnification the cells are polygonal with variably distinct borders, a pale eosinophilic and vacuolated cytoplasm, and a round vesiculate nucleus with dispersed chromatin. Leptomeninges were found to be rarely compromised with all tumors remaining in the epidural space. H & E , original magnification ×4 *(upper left)*, × 10 *(upper right)*, and × 40 *(lower)*.

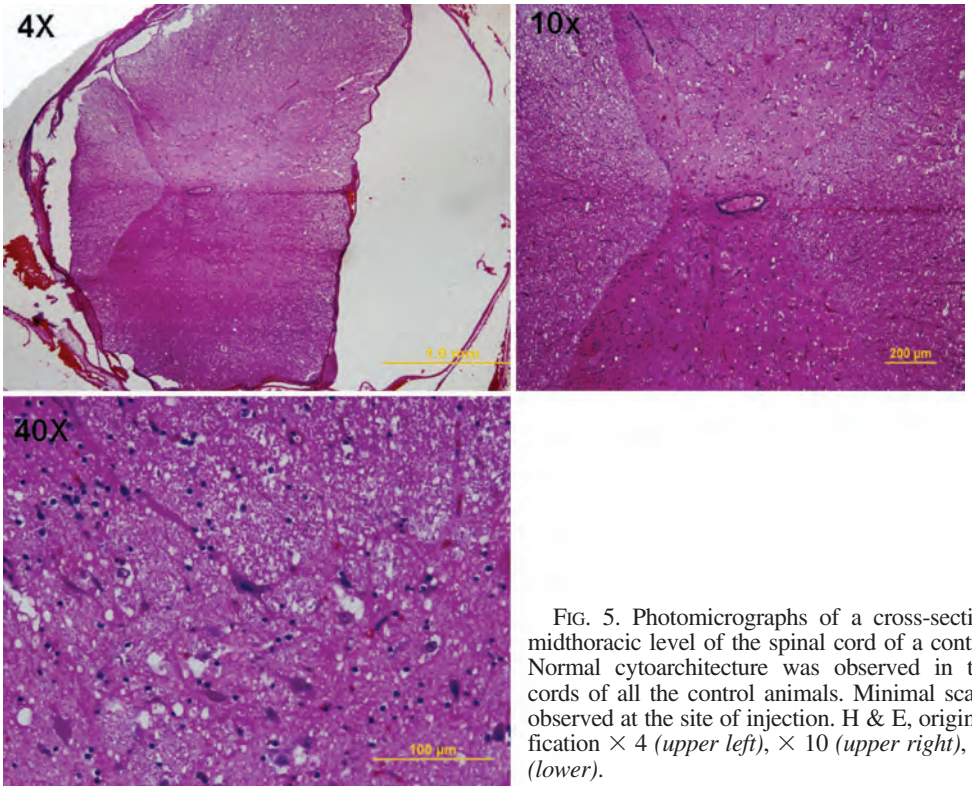

FIG. 5. Photomicrographs of a cross-section at the midthoracic level of the spinal cord of a control rabbit. Normal cytoarchitecture was observed in the spinal cords of all the control animals. Minimal scarring was observed at the site of injection. H & E, original magnification × 4 *(upper left)*, × 10 *(upper right)*, and × 40 *(lower)*.

References

1. Allen JC, Aviner S, Yates AJ, Boyett JM, Cherlow JM, Turski PA, et al: Treatment of high-grade spinal cord astrocytoma of childhood with "8-in-1" chemotherapy and radiotherapy: a pilot study of CCG-945. Children's Cancer Group. **J Neurosurg 88:** 215–220, 1998
2. Boehm T, Malich A, Reichenbach JR, Fleck M, Kaiser WA: Percutaneous radiofrequency (RF) thermal ablation of rabbit tumors embedded in fat: a model for RF ablation of breast tumors. **Invest Radiol 36:**480–486, 2001
3. Bouffet E, Amat D, Devaux Y, Desuzinges C: Chemotherapy for spinal cord astrocytoma. **Med Pediatr Oncol 29:**560–562, 1997
4. Bowers DC, Weprin BE: Intramedullary spinal cord tumors. **Curr Treat Options Neurol 5:**207–212, 2003
5. Carson BS, Anderson JH, Grossman SA, Hilton J, White CL III, Colvin OM, et al: Improved rabbit brain tumor model amenable to diagnostic radiographic procedures. **Neurosurgery 11:**603–608, 1982
6. Constantini S, Miller DC, Allen JC, Rorke LB, Freed D, Epstein FJ: Radical excision of intramedullary spinal cord tumors: surgical morbidity and long-term follow-up evaluation in 164 children and young adults. **J Neurosurg (Spine 2) 93:**183–193, 2000
7. Cooper PR, Epstein F: Radical resection of intramedullary spinal cord tumors in adults. Recent experience in 29 patients. **J Neurosurg 63:**492–499, 1985
8. Epstein FJ, Farmer JP, Freed D: Adult intramedullary astrocytomas of the spinal cord. **J Neurosurg 77:**355–359, 1992
9. Epstein FJ, Farmer JP, Freed D: Adult intramedullary spinal cord ependymomas: the result of surgery in 38 patients. **J Neurosurg 79:**204–209, 1993
10. Farrell CL, Stewart PA, Del Maestro RF: A new glioma model in rat: the C6 spheroid implantation technique permeability and vascular characterization. **J Neurooncol 4:**403–415, 1987
11. Foreman NK, Hay TC, Handler M: Chemotherapy for spinal cord astrocytoma. **Med Pediatr Oncol 30:**311–312, 1998
12. Goldberg SN, Gazelle GS, Compton CC, Mueller PR, McLoud TC: Radio-frequency tissue ablation of VX2 tumor nodules in the rabbit lung. **Acad Radiol 3:**929–935, 1996
13. Goldberg SN, Walovitch RC, Straub JA, Shore MT, Gazelle GS: Radio-frequency-induced coagulation necrosis in rabbits: immediate detection at US with a synthetic microsphere contrast agent. **Radiology 213:**438–444, 1999
14. Griffitt W, Glick RP, Lichtor T, Haughton DE, Cohen EP: Development of a new mouse brain tumor model using implantable micro-cannulas. **J Neurooncol 41:**117–120, 1999
15. Guerin C, Olivi A, Weingart JD, Lawson HC, Brem H: Recent advances in brain tumor therapy: local intracerebral drug delivery by polymers. **Invest New Drugs 22:**27–37, 2004
16. Henson JW, Thornton AF, Louis DN: Spinal cord astrocytoma: response to PCV chemotherapy. **Neurology 54:**518–520, 2000
17. Hoang-Xuan K, Capelle L, Kujas M, Taillibert S, Duffau H, Lejeune J, et al: Temozolomide as initial treatment for adults with low-grade oligodendrogliomas or oligoastrocytomas and correlation with chromosome 1p deletions. **J Clin Oncol 22:** 3133–3138, 2004
18. Jallo GI, Danish S, Velasquez L, Epstein F: Intramedullary low-grade astrocytomas: long-term outcome following radical surgery. **J Neurooncol 53:**61–66, 2001
19. Jallo GI, Freed D, Epstein FJ: Spinal cord gangliogliomas: a review of 56 patients. **J Neurooncol 68:**71–77, 2004
20. Kidd JG, Rous P: A transplantable rabbit carcinoma originating in a virus-induced papilloma and containing the virus in masked or altered form. **J Exp Med 71:**813–838, 1940
21. Lee FT Jr, Chosy SG, Naidu SG, Goldfarb S, Weichert JP, Bakan DA, et al: CT depiction of experimental liver tumors: contrast enhancement with hepatocyte-selective iodinated triglyceride versus conventional techniques. **Radiology 203:**465–470, 1997
22. Lonjon M, Goh KY, Epstein FJ: Intramedullary spinal cord ependymomas in children: treatment, results and follow-up. **Pediatr Neurosurg 29:**178–183, 1998
23. Lowis SP, Pizer BL, Coakham H, Nelson RJ, Bouffet E: Chemotherapy for spinal cord astrocytoma: can natural history be modified? **Childs Nerv Syst 14:**317–321, 1998
24. Rand RW, Snow HD, Elliott DG, Bubbers JE, Barbaric ZL, Brown WJ: Thermo-magnetic surgery for experimental renal cancer. **J Urol 128:**618–620, 1982
25. Salcman M, Botero E, Rao KC, Broadwell RD, Scott E: Intramedullary canine spinal cord tumor model. **J Neurosurg 61:** 761–766, 1984
26. Salcman M, Scott EW, Schepp RS, Knipp HC, Broadwell RD: Transplantable canine glioma model for use in experimental neuro-oncology. **Neurosurgery 11:**372–381, 1982
27. Sandalcioglu IE, Gasser T, Asgari S, Lazorisak A, Engelhorn T, Egelhof T, et al: Functional outcome after surgical treatment of intramedullary spinal cord tumors: experience with 78 patients. **Spinal Cord 43:**34–41, 2005
28. Weizsaecker M, Deen DF, Rosenblum ML, Hoshino T, Gutin PH, Barker M: The 9L rat brain tumor: description and application of an animal model. **J Neurol 224:**183–192, 1981

Manuscript received January 13, 2005.
Accepted in final form May 23, 2005.
This work was partially funded through a generous gift from the Malia's C.O.R.D. Foundation.

Address reprint requests to: George Jallo, M.D., Department of Neurosurgery, The Johns Hopkins Hospital, Harvey 811, 600 North Wolfe Street, Baltimore, Maryland 21287. email: gjallo1@jhmi.edu.